crystals

MDPI

Article

A Novel Substrate-Binding Site in the X-ray Structure of an Oxidized *E. coli* Glyceraldehyde 3-Phosphate Dehydrogenase Elucidated by Single-Wavelength Anomalous Dispersion

Rodríguez-Hernández Annia [1,*], Enrique Romo-Arévalo [2] and Adela Rodríguez-Romero [1,*]

[1] Instituto de Química, Universidad Nacional Autónoma de México, Circuito Exterior s/n, Ciudad Universitaria, Coyoacán, 04510 Ciudad de México, Mexico
[2] Facultad de Odontogía, Universidad Nacional Autónoma de México, Investigación Científica 1853, Ciudad Universitaria, 04360 Ciudad de México, Mexico; dr_roaren@yahoo.com.mx
* Correspondence: arodriguezh@iquimica.unam.mx (R.-H.A.); adela@unam.mx (A.R.-R.)

Received: 31 October 2019; Accepted: 22 November 2019; Published: 26 November 2019

Abstract: *Escherichia coli* (*E. coli*), one of the most frequently used host for the expression of recombinant proteins, is often affected by the toxic effect of the exogenous proteins that is required to express. Glyceraldehyde 3-phosphate dehydrogenase (GAPDH) is a multi-functional protein that has been used as a control marker for basal function and it is known to undergo cysteine oxidation under different types of cellular stress. Here, we report the 3D structure of the endogenous GAPDH purified from stressed *E. coli* cells expressing a eukaryotic protein. The structure was solved at 1.64 Å using single-wavelength anomalous dispersion (SAD) phasing with a selenium-modified enzyme. Interestingly, each GAPDH monomer contains a molecule of glyceraldehyde-3 phosphate in a non-previously identified site. Furthermore, the catalytic Cys149 is covalently attached to a ~300 Da molecule, possibly glutathione. This modification alters the conformation of an adjacent alpha helix in the catalytic domain, right opposite to the NAD^+ binding site. The conformation of the alpha helix is stabilized after soaking the crystals with NAD^+. These results exemplify the effects that the overexpression of an exogenous protein has over the host proteins and sheds light on the structural changes that large oxidant molecules on the catalytic cysteine produce for the GAPDH enzyme.

Keywords: cysteine oxidation; glyceraldehyde 3-phosphate dehydrogenase; glutathione; glyceraldehyde 3-phosphate; Single-Wavelength Anomalous Dispersion (SAD); X-ray diffraction

1. Introduction

Glyceraldehyde 3-phosphate dehydrogenase (GAPDH) is a ubiquitous, highly studied enzyme that reversibly transforms glyceraldehyde 3-phosphate to 1,3-diphosphoglycerate in the presence of NAD^+ and inorganic phosphate in the glycolysis pathway [1]. Due to its central participation in glycolysis and its high abundance, it is considered a biological marker of basal activity [2,3]. Nonetheless, apart from its glycolytic function, GAPDH displays a battery of moonlighting activities. In eukaryotic organisms, it participates in membrane transport, DNA repair and replication, autophagy, pathogenesis, host immunosuppression, and microtubule building, among others [4–8]. In bacteria, several protein-binding partners have been identified for GAPDH, suggesting its participation in a variety of non-canonical functions, similar to the ones described in eukaryotes [9]. Bacterial GAPDH is known to act as a virulence factor in pathogens [10–12], it is secreted in probiotics like *Lactobacillus plantarum* [13], and participates in DNA repair, being one component of a complex of proteins dedicated to this end [14].

GAPDH is a redox-regulated protein, and the regulation of its functions is mediated mainly by the reduction and oxidation of cysteine residues. This enzyme is one of the three cellular proteins known to first undergo S-thiolation under oxidative stress conditions [15,16], which in human cells target GAPDH to the nucleus and initiate a metabolic pathway that leads to apoptosis [7]. Thus, the stress to which cells are exposed modulates the moonlighting functions of GAPDH and promotes changes in its oligomeric state, cellular localization, and/or post-translational modifications [5,17]. The later play a primordial role in the activity modulation of GAPDH and also contribute to changes in its oligomeric state [18] and cellular localization [17]. For instance, the primary location of the tetrameric GAPDH is in the cytoplasm, where it conducts its canonical role in glycolysis. However, when the cell is exposed to high levels of H_2O_2, GAPDH is irreversibly inhibited presumably by the formation of sulphenic acid in the active site cysteine [19], becoming a switch that balances the equilibrium between the glycolytic cycle and the pentose phosphate metabolic pathway and promoting the formation of NADPH to combat ROS-produced cell stress [17,20]. Hydrogen peroxide-induced oxidation of human GAPDH also enhances glutathionylation both in vivo and in vitro, perhaps increasing the availability of the glutathionylation site by a conformational change [15,19].

GAPDH posttranslational modifications such as acetylation, phosphorylation, S-nitrosylation, S-thiolation, sulphonation, glutathionylation, O-GlcNacylation, CoAlation, S-bacillithiolation, and others have been broadly studied in different organisms [17–19,21–24]. However, only a few studies have reported a relationship between post-translational modifications and conformational changes in the enzyme, which could also produce its re-direction to alternative functions [18,25]. S-glutathionylation was proposed to change the structure of GAPDH, affecting its regulation inside the cell [15]. Nonetheless, such change remains elusive.

In this study, we obtained the crystallographic 3D structure of native *E. coli* GAPDH (EcGAPDH) purified from cells over-expressing a human protein. The EcGAPDH was modified at the catalytic Cys149 promoting an alternative conformation of an alpha helix in the catalytic domain, comprised by residues 206 to 214. The structure also disclosed a novel-binding site for the substrate glyceraldehyde 3-phosphate. To the best of our knowledge, there is no previous information regarding a secondary site for the substrate, and we ignore if this may have metabolic or functional implications in this or other systems. Finally, the soaking of the GAPDH crystals in the presence of the coenzyme NAD^+ stabilized the secondary conformation of the alpha helix. Our results provide novel remarkable conformational changes in GAPDH that seem to be related to its non-glycolytic functions and continue to demonstrate the difficulty of understanding the roles and mechanisms of this multi-functional macromolecule.

2. Materials and Methods

2.1. Preparation of EcGAPDH

EcGAPDH was purified from BL21(DE3) *E. coli* cells (Merck Millipore, KGaA, Darmstadt, Germany) transformed with a pET28a (+) vector, carrying a synthetic *E. coli* codon optimized sequence of a human gene that codifies for a 32.4 kDa protein (GeneScript, New Jersey, US). An initial overnight culture containing 100 µg/mL ampicillin (Sigma-Aldrich, St. Louis, Mo, US) was grown during 16 h at 37 °C with constant shaking at 200 rpm. The cell pellet from this culture was recovered by centrifugation for 5 min at 4500 g and resuspended in 1 L of sterile LB-Miller (Sigma-Aldrich, St. Louis, Mo, US) or homemade M9 media. To prepare the M9 media, we dissolved 64 g of Na_2HPO_4 7·H_2O, 15 g KH_2PO_4, 2.5 g of NaCl and 5 g of NH_4Cl in 1 L of distilled H_2O and sterilized (M9 salts). Then, 200 mL of the sterile M9 salts and 2 mL of filtered-sterilized 1M $MgSO_4$, 20 mL of 20% glucose and 100 µl of 1M $CaCl_2$ were added, and the volume was brought out to 1 L with distilled H_2O.

The cultures were grown at 37 °C in constant agitation at 200 rpm until the optical density at 600 nm reached 0.4. Then, for the LB-miller media, we induced the expression of the human protein cloned in the pET28a (+) vector (HACD1 gene) by adding 1mM Isopropyl β- d-1-thiogalactopyranoside (IPTG). In the case of the minimal media, 50 mg of selenomethionine, 100 mg of lysine, 100 mg

threonine, 100 mg phenylalanine, 50 mg leucine, 50 mg isoleucine and 50 mg of valine were added, and after 15 min of incubation with the additives, we induced protein expression with 1 mM IPTG. Both cultures were allowed to grow during 14 h at 18 °C, and cell pellets from the cultures were recovered by centrifugation at 6400 g.

2.2. Protein Purification

Cell pellets were resuspended in lysis buffer containing 20 mM Na_2HPO_4, 50 mM NaCl, one tablet of complete protease (Roche Diagnostics, Indianapolis, IN, USA) and 1 mM PMSF (Amresco, Solon, OH, USA) at pH 7.2. The cell suspension was disrupted by sonication for eight minutes on ice, and the lysate was centrifuged 45 min at 20,000 g. The supernatant was filtered two times before chromatography, first with a 0.45 µm PVDF membrane and then with a 0.22 µm PVDF membrane (Merck Millipore, KGaA, Darmstadt, Germany). The filtered lysate was loaded onto a hydroxyapatite column equilibrated in with 20 mM Na-phosphate buffer pH 6.8, the column was washed using the same buffer and the protein was eluted with a linear gradient from 20 mM to 500 mM Na-phosphate buffer pH 6.8 and 50 mM NaCl. The fractions containing more protein were passed through an affinity His prep FF 16/10 column pre-equilibrated with 5 mM imidazole and 50 mM NaCl, washes contained 50 mM NaCl and 50, 100, or 250 mM imidazole each, the protein eluted at 100 mM imidazole. After affinity chromatography, the protein was concentrated and loaded onto a molecular filtration S100 column equilibrated in 10 mM HEPES pH 6.8 and 20 mM NaCl. Fractions containing the purest protein were concentrated and used for dynamic light scattering (DLS), circular dichroism (CD), and crystallization experiments.

2.3. Crystallization

Initial crystallization conditions were carried out with crystal screens I and II (Hampton Research Aliso Viejo, CA, US) and Nextal PACT Suite (Qiagen, Germantown, MD, US) with the native, non-modified enzyme at a final concentration of 5.5 mg/mL in 10 mM HEPES pH 7.2. The crystallization trays were incubated at 18 °C. After six days of incubation, several conditions contained crystals, but only two of these resulted promising D2 from CSI and H11 from PACT the Suite. The best crystals were obtained in the optimized conditions from CSI, contained 0.1 M HEPES pH 7.5 and 1.43 M sodium citrate, and grew after three days of incubation. The selenium-modified protein was crystallized using only the optimized crystallization conditions identical to those of the native enzyme.

2.4. Soaking Experiments

Crystals from the selenium modified enzyme grown in the optimum crystallization conditions, were soaked for 10 min in 5 mM NAD^+ dissolved in mother liquor; one crystal was then cryo-protected with mother liquor and 25% trehalose and collected in the in-house X-ray diffractometer at the Laboratorio Nacional de Estructura de Macromoléculas (LANEM-IQ-UNAM).

2.5. Data Collection and Processing

The two Se-modified protein crystal were cryo-protected with 25% trehalose, 0.1 M HEPES pH 7.5, and 1.43 M sodium citrate. In the case of the native protein, the cryo-protectant solution contained 30% glycerol and all the other components of the mother liquor. All crystals were frozen directly in the cryo-stream and used to collect a complete dataset. For the Se-modified crystals, one data set was collected in order to obtain high redundancy for SAD phasing. Data collection was performed at LANEM-IQ-UNAM with a Rigaku MicroMax-007HF rotating anode and a Dectris Pilatus3R 200K-A detector (Rigaku, The Woodlands, TX, US). Data were processed using HKL3000 [26], and the spatial group was revised with the program Pointless from CCP4 [27]. The .mtz file from pointless was then used in AutoSol (Phenix) [28] to obtain the phases. Initial modeling was done automatically with ArpWarp (CCP4) [27], followed by manual modeling using Coot [29].

2.6. Model Refinement

The quality of the diffraction data and the presence of Se in the protein allowed us to obtain a model using SAD. AutoSol (Phenix) gave an initial result for the phase. Manual modeling allowed us to finish the construction of one monomer, and the sequence of the model was blasted (Protein-BLAST) to determine the identity of the protein. GAPDH from *E. coli* was the main hit. Refinement was continued, and we discovered the presence of three main positive, unknown electron density blobs. We used LigandFit from Phenix to identify the ligands, which were trehalose (TRE) and glyceraldehyde 3-phosphate (G3P). Glutathione (GSH) was manually built; however, despite our attempts, we could not achieve a good fit to the electron density map. All ligands were built using coot and the .CIF files from the CCP4 library. To obtain a model with two conformations in an entire alpha helix, the last steps of model refinement were done using two individual models, for each model one of the two observed conformations for residues 206–214 (Ser, Ser, Thr, Gly, Ala, Ala, Lys, Ala, Val) were used. The coordinates for the residues comprising this alpha helix were merged in a single model, given occupancy of 0.5 and refined. To obtain the GAPDH models for the native protein, and from the soaking experiment, we used the final model from the Se-modified protein during molecular replacement (MR) using Phaser-MR from Phenix [30]. Removal of all solvent molecules, ligands, and the alpha helix comprised by 206–214 was performed before MR. The models were refined using Phenix.refine [31], and the missing residues were added manually according to the observed electron density using Coot [29]. Final models were validated and deposited in the PDB database (6UTO, 6UTN, and 6UTM).

2.7. PDB Search and Comparison

The Protein Data Bank was used to find all the available structures of GAPDH. Employing the sequence from the *E. coli* enzyme, an initial hit of 171 entries was obtained. From these, manual inspection allowed us to remove 11 structures, which corresponded to other enzymes, then a set of 160 models was analyzed. The presence of ligands and their location in the structure was obtained from visual inspection using Coot and from the PDB entries.

2.8. Matrix-Assisted Laser Desorption/Ionization-Time of Flight (MALDI-TOF)

We determined the mass of EcGAPDH from the protein contained in three crystals from the native and three crystals from the Se-modified protein, separately. Sinapinic acid was used as matrix and was added directly to the crystals, which were loaded onto a MALDI plate. Matrix-assisted laser desorption/ionization-time of flight (MALDI-TOF) was performed in a Microflex Bruker instrument (Bruker, Billerica, MA, US), with a nitrogen laser at a wavelength of 337 nm, with positive polarity and acceleration of 20 kV using the linear acquisition operation. Here, 1000 shots were used to collect the spectrums. Bovine serum albumin (66,431 Da) and a chitinase from agave (31,742.10 Da) [32] were used as calibration markers.

3. Results

3.1. Crystals

After six days, crystals grew to maximum dimensions of 300 μm × 200 μm. Characterization of the crystals showed that they diffracted X-rays to a maximum of 1.64 Å and belonged to the space group C2221, with unit cell dimensions of a = 77.273, b = 186.709, c = 122.132, and $\alpha = \beta = \gamma = 90$ (Table 1). All crystals contained two GAPDH monomers in the asymmetric unit with a Matthews' coefficient of 2.08 $Å^3Da^{-1}$ and a solvent content of 40.80%. The GAPDH dimer forms a tetramer with symmetry-related molecules. Three crystallographic structures were solved—one for a Se-modified enzyme, one for the native enzyme, and one for the Se-modified enzyme soaked in NAD^+.

Table 1. Data collection and refinement statistics.

Parameter	Se-Modified	Se-Modified NAD^+	Native
Data collection			
Wavelength (Å)	1.54	1.54	1.54
Space group	C2221	C2221	C2221
	77.27	77.67	77.91
Cell dimensions a, b, c (Å)	186.71	187.35	186.97
	122.13	121.67	121.75
Resolution range (Å)	50–1.64	38.8–1.79	46.7–2.14
Outer shell	1.67–1.64	1.82–1.79	2.17–2.14
Total reflections	1,157,097	746,389	48,546
Unique reflections	107,066	83,268	14,278
Completeness (%)	99.6 (84.5)	99.8 (99.1)	97.9 (89.3)
Multiplicity	11.6 (6.7)	9.0 (6.3)	3.4 (2.0)
Mean I/σ(I)	44.7 (2.7)	37.7 (3.0)	31.3 (2.4)
R_{merge}	0.76 (0.05)	0.73 (0.11)	0.29 (.078)
R_{meas}	0.82 (0.06)	0.80 (0.12)	0.37 (0.09)
R_{pim}	0.31 (0.02)	0.31 (0.036)	
Wilson B-factor ($Å^2$)	15.0	16.3	28.4
CC1/2 (high resolution shell)	0.86	0.87	0.86
Refinement			
R_{work}/R_{free}	0.17/0.19	0.18/0.20	0.16/0.20
Average B, all atoms ($Å^2$)	16.7	21.0	31.0
Total atoms	5825	5598	5373
Protein	5126	4981	4989
Ligands	71	71	35
Water	628	546	349
R.m.s. deviations			
Bond lengths (Å)	0.008	0.015	0.009
Bond angles (°)	1.040	1.324	1.034
Ramachandran plot			
Favored (%)	96.04	96.31	95.43
Allowed (%)	3.66	3.38	4.12
Outliers (%)	0.30	0.31	0.46
PDB entry	6UTO	6UTN	6UTM

3.2. Identification of GAPDH

For this study, our initial intention was to express a human protein with a molecular mass of 32.4 kDa in *E. coli* cells (see methods). Instead, we purified an endogenous protein from the bacteria, which we determined to be homogeneous using DLS, and to be folded with a CD spectrum in the far-UV region (data not shown). Therefore, we conducted the crystallization experiments, and suitable crystals grew after six days at 18 °C. The selenium modified protein was prepared and crystallized to obtain the experimental phases. However, when we analyzed the partial sequence of the model built with ArpWarp and Coot, it did not match the sequence of the initial target protein; thus, suggesting the presence of a different protein in the crystals. A MALDI-TOF spectrum was obtained using three crystals from the native, non-modified protein, and the mass corresponded to 35.5 kDa (Figure 1). Finally, the complete protein sequence and its identity were obtained from the experimental model obtained using SAD and BLAST (NCBI), respectively.

3.3. GAPDH Structures

Once that we identified GAPDH in the Se-modified crystal and obtained a refined model, we determined the three-dimensional structure of EcGAPDH from the native and NAD^+ crystals. Overall, the structure of GAPDH is considerably similar in the three crystals. Superposition between the native and Se-modified crystals gives an RMSD of 0.16 Å, whereas the RMSD between the Se-modified model and the Se-modified crystal soaked in NAD^+ is 0.15 Å. Thus, there are no global differences in the overall structures. In the three cases, there is a dimer in the asymmetric unit, and GAPDH

forms a crystallographic tetramer with symmetry related molecules (Figure 2a). Two domains compose EcGAPDH, the NAD^+ binding domain, residues 1–148, 312–330 (*E. coli* numbering) and the catalytic domain, residues 148–311 [1,33,34]. The NAD^+ binding domain consist of six parallel and one anti-parallel β-strands, surrounded by four α-helices, the typical structure of a Rossmann fold. Residues from two subunits form the NAD^+ binding site, in one monomer residues Gly10, Arg11, Ile12, Asp33, and Asn313 have close contacts with the NAD^+ molecule, nonetheless residues Gly187 and Pro188 from the adjacent monomer are near the cofactor (~4.2–5.0 Å). A sheet of seven anti-parallel β-strands and four α-helices (residues 149–165, 209–216, 250–265, and 313–330) form the catalytic domain. At the beginning of the first α-helix, residues Cys149 and His176 constitute the catalytic site in EcGAPDH. Helix 149–165 is adjacent to the α-helix formed by residues 209–216 and both the catalytic Cys149 and the later helix are right opposite to the NAD^+ binding region (Figure 2b).

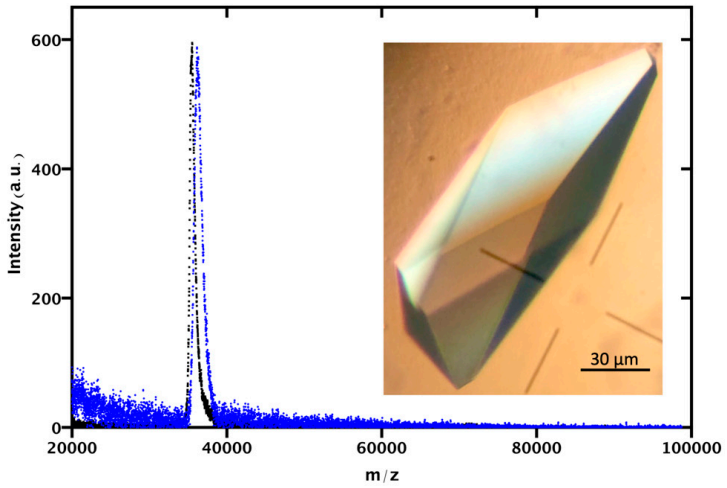

Figure 1. Matrix-assisted laser desorption/ionization-time of flight (MALDI-TOF) and glyceraldehyde 3-phosphate dehydrogenase (GAPDH) crystals. The mass of non-modified GAPDH (35.50 kDa, black) and Se-modified GAPDH with oxidant molecule (36.14 kDa, blue) was obtained from GAPDH crystals. The mass difference suggests the presence of one GSH and 7 Se-methionines per GAPDH monomer. Inset, native GADPH crystal.

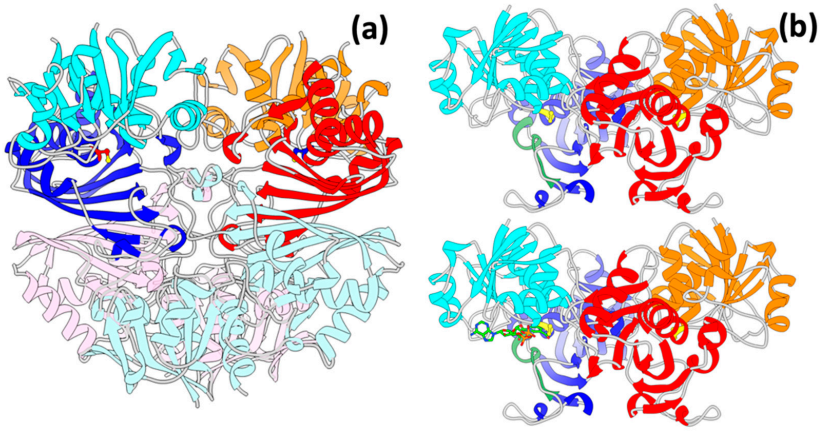

Figure 2. Three-dimensional structure of GAPDH. (**a**) A homodimer was crystallized in the asymmetric unit (darker colors), a tetramer is formed by symmetry molecules (light colors). Each GAPDH monomer is composed of two domains, the NAD^+ binding domain (residues 1–148 and 312–330) is shown in cyan and orange on individual monomers, whereas the catalytic domain (residues 149–311) is shown in blue and red. (**b**) The NAD^+ (in sticks) binding site and the catalytic site (yellow) are adjacent to the helix that changes its conformation (shown in green only in the left monomers). NAD^+ was superimposed in this model using chain C from PDB 4mvj (**b**, bottom left).

3.4. Oxidized Cys149 in the GAPDH Model

A quick analysis of the electron density maps in the Se-modified crystal revealed several interesting sites with bulky positive electron density in the Fo-Fc map. Notably, a large blob that seemed to be bound to the catalytic Cys149 caught our attention (Figure 3a). After the first rounds of refinement, an initial search for a possible transition state intermediate was unsuccessful; therefore, we searched for other molecules that could oxidize the enzyme. Since the positive density was large, one of the best possible explanations to occupy this density was glutathione (GSH) [35,36]. The molecule was manually modeled with the GSH.CIF file from CCP4. J ligand (coot) was used to build sections of the GSH that better fitted to the density map, and finally, the entire GSH was modeled. The use of GSH gave the best R_{free} and R_{work} values for the model; nevertheless, despite our attempts several clashes between the GSH and the protein were present (Figure S1), thus we decided to remove the GSH from the final model (6UTO). Therefore, a large positive electron density is observed in the Fo-Fc maps (Figure 3a,b). Positive electron density for the modification near Cys149 was observed in two of the three structures obtained in this study, those with the Se-modified protein and the native, non-modified protein. However, the Fo-Fc map electron density for the native crystal was weaker than the one observed for the Se-modified protein. Only the crystals soaked in NAD^+ showed a significant reduction in the electron density surrounding Cys149; in this case, the residue was modeled as a cysteine sufinic acid (Figure 4b). These results suggest that the presence of the exogenic plasmid or the expression of the human protein could have produced the oxidation of the Cys149; however, the stress caused by the use of minimum media, increased the number of modified EcGAPDH, this data is in agreement with the higher amount of stress observed in *E. coli* during the expression of recombinant proteins [37]. To characterize the identity of the modification in Cys149, we performed MALDI-TOF experiments. The native non-modified protein crystals displayed a mass of 35,506.7 Da, and for the Se-modified protein crystals a mass of 36,142.0 Da was obtained, a difference of 635.3 Da is observed, suggesting the presence of one GSH and seven Se-methionines per GAPDH monomer (Figure 1).

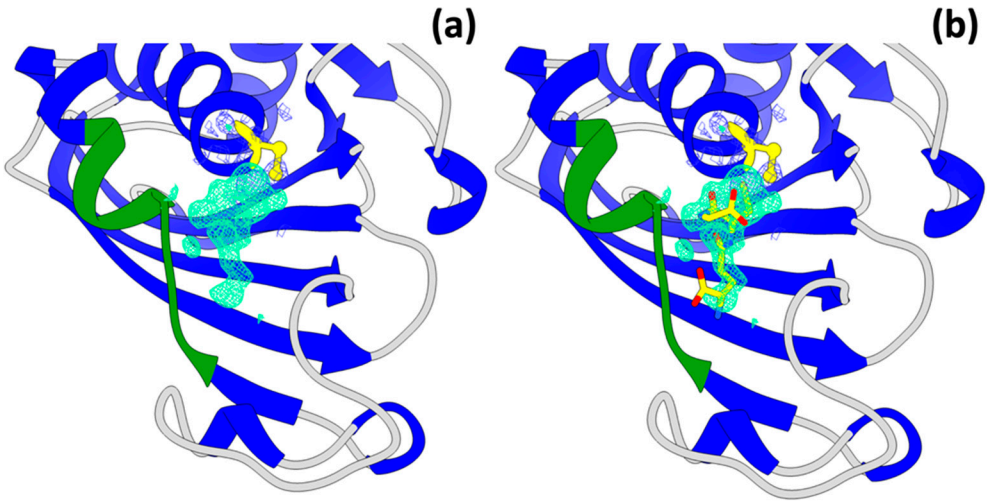

Figure 3. Electron density in the catalytic cysteine. (**a**) The Se-modified GAPDH displayed a large electron density surrounding the catalytic Cys149, the images show a mesh in cyan the Fo-Fc map (σ level 3.0) and a dark blue mesh for the 2Fo-Fc map (σ level 1.0) after final model refinement. (**b**) A likely oxidizer of the GAPDH enzyme is glutathione; nevertheless, it was removed from the final model due to clashes with the protein.

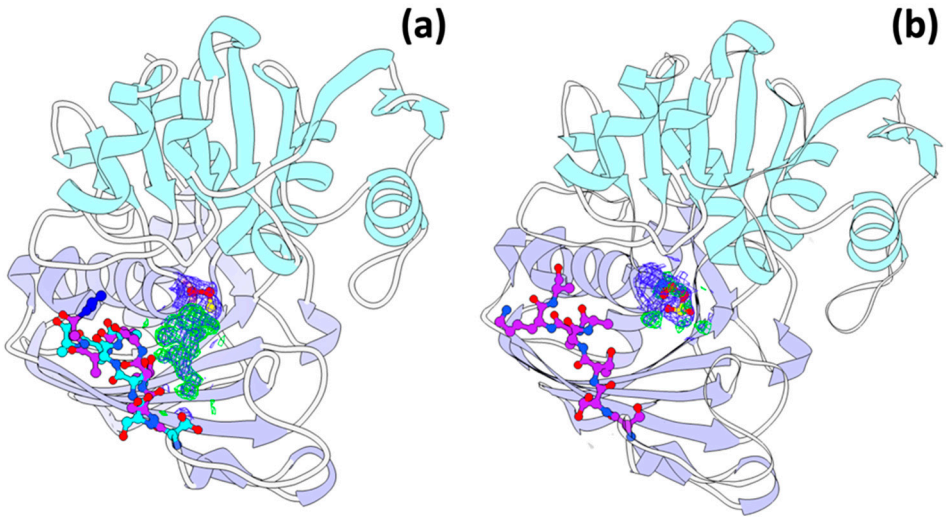

Figure 4. Double conformation of residues 206–214 in the catalytic site of GAPDH. (**a**) A double conformation of residues 206–214 is observed in the GAPDH structure with Se-methionines (cyan and purple). This structure contains a large electron density attached to the catalytic cysteine Cys149 (Fo-Fc map in green). (**b**). One conformation is stabilized for residues 206–214. When the crystals are soaked in a NAD^+ solution (purple), the electron density for the surroundings of Cys149 disappears (Fo-Fc map green mesh).

3.5. Double Conformation of the Helix (Residues 206–214)

During model refinement, some residues of the alpha-helix adjacent to the catalytic site (res. 204–214) displayed positive electron density in their surroundings. The positive density suggested the existence of two conformations for these residues; phenomenon that only occurred when the catalytic Cys149 exhibits a large electron density in its surroundings (native and Se-modified models, PDBs 6UTM, 6UTO). Occupancies for one or the other conformer for each of the nine residues refined to values of 0.59 and 0.41, thus supporting the presence of the two simultaneous conformers. This protein region is relevant since Thr208 and Gly209, participate in the recognition of G3P in the binding site. The large electron density observed in our maps occupies the GP3 binding site, and it was expected that the residues around this site should move to avoid clashing. Interestingly, soaking the crystals with NAD^+ highly reduces the presence of the large electron density around Cys149 and stabilizes the secondary structure of the alpha helix in only one conformation (Figure 4a,b). All residues recovered the conformation previously reported in other EcG3PDH models [33,34,38,39].

3.6. A New Binding Site for Glyceraldehyde 3-Phosphate

In EcGAPDH, residues 148–150 and 208–209 are important for G3P substrate binding, including residues Cys149, and His176, which comprise the catalytic site. After examination of the electron density map, we realized that there was no ligand in the binding pocket. Interestingly, the glyceraldehyde 3-phosphate substrate was found outside the binding site (Figure 5a,b). The density map (2Fo-Fc) showed a complete G3P molecule for monomer A and slightly less electron density for the ligand in monomer B. The phosphate group of G3P interacts with the main chain nitrogen from residues Gly132, Phe135 and Asp136, and also makes a hydrogen bond with the carboxylate oxygen of Asp136 in the NAD^+ binding domain. The glycerol moiety of G3P is almost completely exposed to the solvent and has no contact with symmetry molecules (Figure 5a). To compare our models with other GAPDH structures in the presence of G3P we made a search in the PDB database using the sequence from the *E. coli* GAPDH, which resulted in 160 GAPDHs from which 14 structures belong to the *E. coli* GAPDH. Careful analysis of these models, their ligands and the differences in conformation in the regions reported here was performed. From the 160 GAPDH structures analyzed, 10 contained G3P or an analog, which was present only in the active site of the enzyme. The 14 EcGAPDH models deposited

in the PDB were superimposed with the ones obtained here, and we observed that two structures had a sulfate ion in the same place where G3P is bound in our models (PDBs 1s7c and 5za0).

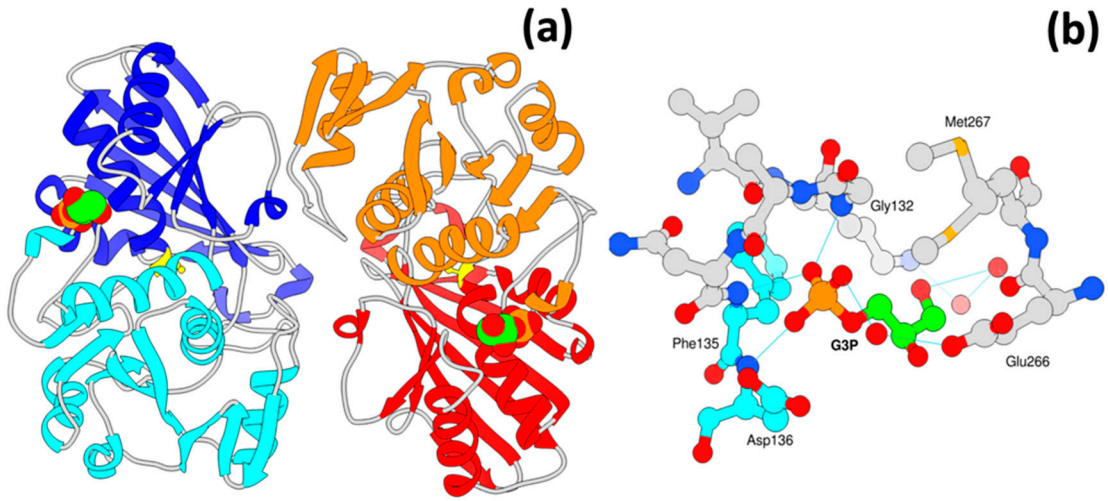

Figure 5. New binding site for glyceraldehyde 3 phosphate (G3P). (**a**) A shallow binding site on the GAPDH surface was found for the GAPDH substrate, the glycerol moiety of G3P (ball representation) is completely exposed to solvent, and no symmetry related molecules are near to the site. (**b**) G3P is anchored to the enzyme mainly through main chain interactions, and only one residue Glu266 interacts indirectly with its side chain and a solvent molecule with one phosphate oxygen of G3P.

Interestingly, from all EcGAPDHs models deposited in the PDB, only ours exhibit a different conformation of Met267 in monomer A (Figure 5b). This conformation creates a small cleft were the G3P binds, and seems to stabilize G3P binding, in contrast with monomer B where the conformation of this methionine is the same as the one present in all other *E. coli* models, in this case, less electron density for the ligand is observed. To the best of our knowledge, this is the first GAPDH structure with a large modification in the catalytic Cys149 and the only one with G3P bound to a non-catalytic site.

3.7. Trehalose Binding Site

Two of the three GAPDH crystals used for X-ray diffraction were soaked for a second in 25% trehalose as cryo-protectant. Nevertheless, the disaccharide bound readily to the enzyme, clear electron density was observed for this molecule in the two models. The binding site for trehalose seems to display some specificity, as it superimposes entirely to one previously observed [33]. There are reports of GAPDH from different organisms binding to other sugars, as this enzyme has been proposed to act as a lectin-like protein [40]. However, the site for sugar-binding has been depicted in only a few works [33], whereas binding studies are much more frequent [40,41].

4. Discussion

Glyceraldehyde 3-phosphate dehydrogenase is one of the most studied enzymes in the last 40 years, and what initially seemed like a simple glycolytic enzyme has been demonstrated to perform crucial roles in metabolism and disease. To date, many of the non-canonical functions of GAPDH are of medical interest because of its involvement in the development of diseases like Alzheimer's and cancer, being part of the oxidative stress response, and also because it can be exploited as a target for vaccine therapeutics [42]. GAPDH is one of the most conserved glycolytic enzymes, displaying between 50–60% identity among different species [1]. Interestingly, while there are several studies about the structure–function relationship of this enzyme regarding its canonical activity, a direct structural connection for the modulation of its non-glycolytic functions is not yet clearly established. Here, we show how a modification of the catalytic Cys149, presumably glutathione, promotes an

unstable conformation of the alpha helix comprised by residues 206 to 214 in the *E. coli* enzyme. The modified GAPDH was obtained from stressed *E. coli* cells overexpressing a human protein and grown in minimum media, as explained in the results section. In our model, the modification of Cys149 does not alter the global structure of the GAPDH nor the helical region where it is located. Nevertheless, it significantly affects the structural stability of the alpha helix adjacent to the catalytic site, moving the entire secondary structure (Figure 4a).

Because the NAD^+ binding domain is close to the catalytic cysteine, NAD^+ soaking experiments were carried out as described in the methods section. To our surprise, the electron density observed for NAD^+ was not enough to accommodate the coenzyme, and the refined occupancy gave a value of 0.7. However, the region comprising residues 206-214 was stabilized in a single conformation (Figure 4b). Some positive electron density was still present in the surroundings of Cys149, though it was only appropriate to model two oxygen atoms for a sulfinic acid derivative (Figure 4b). Superposition of the structures from the NAD^+ soaked crystal and the putative GSH modified EcGAPDH with other reported *E. coli* GAPDHs (PDB entries 2vyn, 1gae, 1gad, 1dc4, 1dc6, 1dc5, 1s7c, 2vyv, 4mvj, 5za0, 6ioj, 6io6, 6io4) showed that this helix is in one predominant conformation in all the structures. Only model 1dc4, which contains a covalently bound transition state G3P displays a similar conformation of the mentioned alpha helix to the one observed for the Se-modified enzyme. It is important to note that only our model displays the two conformations simultaneously. Residues 210-214, from 1dc4, are in a different conformation, which might be attributed to the bulkier moiety attached to Cys149 in our model.

Previously, it has been shown that post-translational modifications can promote changes in the oligomeric state of GAPDH or to promote aggregation [18,25,43,44]. Some modifications modulate the binding partners of GAPDH, and at the same time its participation in different cellular processes. The *E. coli* and *H. sapiens* enzymes share approximately 66% in sequence identity, and only one of the 206–214 residues is not conserved between these two enzymes. This region contains Lys214 (*H. sapiens* numbering, 212 *E. coli*), a crucial residue for the binding of band three transport protein, which is an ion channel in the membrane of erythrocytes, and necessary for the interaction of GAPDH with the membrane [45]. Glutathionylation of GAPDH is a response to oxidative stress in cells that reversibly inactivates the enzyme [19]. Thus, the high abundance of GAPDH has been proposed as a protective anti-oxidative mechanism for the cell, which sometimes promotes its translocation to different compartments and provides alternative functions [46,47]. These findings contribute with structural evidence demonstrating how oxidation of Cys149 induces local conformational changes that could potentially affect binding to other molecules.

To observe a structural effect in the Se-modified crystals, we performed an NAD^+ soaking experiment. Surprisingly, the presence of NAD^+ eliminated the positive electron density near the Cys149. This change also stabilized the secondary structure of the alpha helix, which recovered its commonly observed conformation [33,34,38,39]. However, we could not build the NAD^+ moiety due to its low occupancy (0.7); this data might be in agreement with previous studies in which the affinity towards NAD^+ is decreased for the oxidized enzyme [48]. The presence of NAD^+ in the drop, however, did not affect the presence of G3P in the unusual binding site, which was also present in the native GAPDH obtained from cells overexpressing the human gene. To the best of our knowledge, there is no previous information regarding a secondary site for the substrate, and we ignore if this may have metabolic or functional implications in this or other systems. The residues interacting with the G3P moiety have not been disclosed as particularly important in any other context, and only in two other cases, these same residues were modeled interacting with a sulfate or formate molecule without any apparent significance [33,49]. Therefore, further research is required to investigate the importance of a secondary site and its implications for the GAPDH function. We believe that these results provide information about new remarkable conformational changes in GAPDH that seem to be related to the non-glycolytic functions of *E. coli* GAPDH and which in turn can also be translated to other systems.

5. Conclusions

Cellular stress related to the over-expression of an exogenic protein, and exacerbated by the limited availability of nutrients, promotes modification of the catalytic cysteine of GAPDH in *E. coli* cells. The oxidation of Cys149 alters the conformation of the alpha helix conformed by residues 206–214, which contains a previously identified membrane-binding site of GAPDH [45]. Interaction of the modified enzyme with NAD^+ stabilizes the conformation of the alpha helix and overrides the presence of the oxidizer in the catalytic site. We also identified a new binding site for the substrate G3P in this oxidized protein. None of the residues interacting with the G3P moiety had been previously reported to have any biological relevance. The interaction of the protein with NAD^+ does not affect the binding of G3P in the new site reported. These results might be of importance for the study of non-canonical functions of GAPDH in this and in other homologous systems.

Supplementary Materials: The following is available online at http://www.mdpi.com/2073-4352/9/12/622/s1, Figure S1: Possible interactions of GAPDH and GSH.

Author Contributions: R.-H.A. conceived the idea, performed experiments, analyzed the data, and wrote the manuscript. E.R.-A. performed experiments and reviewed the manuscript. A.R.-R. conceived the idea, performed experiments, analyzed the data, and wrote the manuscript.

Funding: Consejo Nacional de Ciencia y Tecnología: 299048; Dirección General de Asuntos del Personal Académico, Universidad Nacional Autónoma de México: IN208418.

Acknowledgments: We thank Alejandra Hernández-Santoyo for her help during model refinement. This study was founded with CONACYT grant number (Grant 299048 to A.R.-R.) and DGAPA-UNAM-PAPIIT grant number (IN208418 to A.R.-R., IA202618 to E.R.-A.). The authors are thankful to LANEM-IQ-UNAM and to M.C. Georgina Espinosa-Pérez for X-ray data processing. We are also thankful to M.C. Lucero Rios-Ruiz for her assistance in MALDI-TOF acquisition, to Patricia Cano-Sánchez for her continuous support in the use of molecular biology techniques, and to Yan A. García-Hernández for technical assistance.

Conflicts of Interest: The authors declare that the research included in this article was conducted in the absence of commercial or financial interests and generates no conflicts.

References

1. Boyer, P.D. (Ed.) *Oxidation Reduction Part C*; Academic Press, Inc. (London): Cambridge, MA, USA, 1976; Volume XIII.
2. Gustafsson, A.C.; Kupershmidt, I.; Edlundh-Rose, E.; Greco, G.; Serafino, A.; Krasnowska, E.K.; Lundeberg, T.; Bracci-Laudiero, L.; Romano, M.C.; Parasassi, T.; et al. Global gene expression analysis in time series following N-acetyl L-cysteine induced epithelial differentiation of human normal and cancer cells in vitro. *BMC Cancer* **2005**, *5*. [CrossRef] [PubMed]
3. Sirover, M.A. New insights into an old protein: The functional diversity of mammalian glyceraldehyde-3-phosphate dehydrogenase. *BBA Protein Struct. Mol. Enzymol.* **1999**, *1432*, 159–184. [CrossRef]
4. Azam, S.; Jouvet, N.; Jilani, A.; Vongsamphanh, R.; Yang, X.M.; Yang, S.; Ramotar, D. Human Glyceraldehyde-3-phosphate Dehydrogenase Plays a Direct Role in Reactivating Oxidized Forms of the DNA Repair Enzyme APE1. *J. Biol. Chem.* **2008**, *283*, 30632–30641. [CrossRef] [PubMed]
5. Butera, G.; Mullappilly, N.; Masetto, F.; Palmieri, M.; Scupoli, M.T.; Pacchiana, R.; Donadelli, M. Regulation of Autophagy by Nuclear GAPDH and Its Aggregates in Cancer and Neurodegenerative Disorders. *Int. J. Mol. Sci.* **2019**, *20*, 2062. [CrossRef]
6. Butterfield, D.A.; Hardas, S.S.; Lange, M.L.B. Oxidatively Modified Glyceraldehyde-3-Phosphate Dehydrogenase (GAPDH) and Alzheimer's Disease: Many Pathways to Neurodegeneration. *J. Alzheimers Dis.* **2010**, *20*, 369–393. [CrossRef]
7. Dastoor, Z.; Dreyer, J.L. Potential role of nuclear translocation of glyceraldehyde-3-phosphate dehydrogenase in apoptosis and oxidative stress. *J. Cell Sci.* **2001**, *114*, 1643–1653.
8. Heard, K.S.; Diguette, M.; Heard, A.C.; Carruthers, A. Membrane-bound glyceraldehyde-3-phosphate dehydrogenase and multiphasic erythrocyte sugar transport. *Exp. Physiol.* **1998**, *83*, 195–202. [CrossRef]

9. Ferreira, E.; Gimenez, R.; Aguilera, L.; Guzman, K.; Aguilar, J.; Badia, J.; Baldoma, L. Protein interaction studies point to new functions for Escherichia coli glyceraldehyde-3-phosphate dehydrogenase. *Res. Microbiol.* **2013**, *164*, 145–154. [CrossRef]
10. Aguilera, L.; Ferreira, E.; Gimenez, R.; Fernandez, F.J.; Taules, M.; Aguilar, J.; Vega, M.C.; Badia, J.; Baldoma, L. Secretion of the housekeeping protein glyceraldehyde-3-phosphate dehydrogenase by the LEE-encoded type III secretion system in enteropathogenic Escherichia coli. *Int. J. Biochem. Cell B* **2012**, *44*, 955–962. [CrossRef]
11. Lama, A.; Kucknoor, A.; Mundodi, V.; Alderete, J.F. Glyceraldehyde-3-Phosphate Dehydrogenase Is a Surface-Associated, Fibronectin-Binding Protein of Trichomonas vaginalis. *Infect. Immun.* **2009**, *77*, 2703–2711. [CrossRef]
12. Querol-Garcia, J.; Fernandez, F.J.; Marin, A.V.; Gomez, S.; Fulla, D.; Melchor-Tafur, C.; Franco-Hidalgo, V.; Albert, S.; Juanhuix, J.; de Cordoba, S.R.; et al. Crystal Structure of Glyceraldehyde-3-Phosphate Dehydrogenase from the Gram-Positive Bacterial Pathogen A. vaginae, an Immunoevasive Factor that Interacts with the Human C5a Anaphylatoxin. *Front. Microbiol.* **2017**, *8*. [CrossRef]
13. Sanchez, B.; Schmitter, J.M.; Urdaci, M.C. Identification of novel proteins secreted by Lactobacillus rhamnosus GG grown in de Mann-Rogosa-Sharpe broth. *Lett. Appl. Microbiol.* **2009**, *48*, 618–622. [CrossRef]
14. Ferreira, E.; Gimenez, R.; Canas, M.A.; Aguilera, L.; Aguilar, J.; Badia, J.; Baldoma, L. Glyceraldehyde-3-phosphate dehydrogenase is required for efficient repair of cytotoxic DNA lesions in Escherichia coli. *Int. J. Biochem. Cell B* **2015**, *60*, 202–212. [CrossRef]
15. Schuppekoistinen, I.; Moldeus, P.; Bergman, T.; Cotgreave, I.A. S-Thiolation of Human Endothelial-Cell Glyceraldehyde-3-Phosphate Dehydrogenase after Hydrogen-Peroxide Treatment. *Eur. J. Biochem.* **1994**, *221*, 1033–1037. [CrossRef]
16. Shenton, D.; Grant, C.M. Protein S-thiolation targets glycolysis and protein synthesis in response to oxidative stress in the yeast Saccharomyces cerevisiae. *Biochem. J.* **2003**, *374*, 513–519. [CrossRef]
17. Tristan, C.; Shahani, N.; Sedlak, T.W.; Sawa, A. The diverse functions of GAPDH: Views from different subcellular compartments. *Cell. Signal.* **2011**, *23*, 317–323. [CrossRef]
18. Park, J.; Han, D.; Kim, K.; Kang, Y.; Kim, Y. O-GlcNAcylation disrupts glyceraldehyde-3-phosphate dehydrogenase homo-tetramer formation and mediates its nuclear translocation. *BBA Proteins Proteom.* **2009**, *1794*, 254–262. [CrossRef] [PubMed]
19. Lind, C.; Gerdes, R.; Schuppe-Koistinen, I.; Cotgreave, I.A. Studies on the mechanism of oxidative modification of human glyceraldehyde-3-phosphate dehydrogenase by glutathione: Catalysis by glutaredoxin. *Biochem. Biophys. Res. Commun.* **1998**, *247*, 481–486. [CrossRef] [PubMed]
20. Ralser, M.; Wamelink, M.M.; Kowald, A.; Gerisch, B.; Heeren, G.; Struys, E.A.; Klipp, E.; Jakobs, C.; Breitenbach, M.; Lehrach, H.; et al. Dynamic rerouting of the carbohydrate flux is key to counteracting oxidative stress. *J. Biol.* **2007**, *6*, 10. [CrossRef]
21. Aroca, A.; Schneider, M.; Scheibe, R.; Gotor, C.; Romero, L.C. Hydrogen Sulfide Regulates the Cytosolic/Nuclear Partitioning of Glyceraldehyde-3-Phosphate Dehydrogenase by Enhancing its Nuclear Localization. *Plant Cell Physiol.* **2017**, *58*, 983–992. [CrossRef] [PubMed]
22. Piattoni, C.V.; Ferrero, D.M.L.; Dellaferrera, I.; Vegetti, A.; Iglesias, A.A. Cytosolic Glyceraldehyde-3-Phosphate Dehydrogenase Is Phosphorylated during Seed Development. *Front. Plant Sci.* **2017**, *8*. [CrossRef] [PubMed]
23. Imber, M.; Huyen, N.T.T.; Pietrzyk-Brzezinska, A.J.; Loi, V.V.; Hillion, M.; Bernhardt, J.; Tharichen, L.; Kolsek, K.; Saleh, M.; Hamilton, C.J.; et al. Protein S-Bacillithiolation Functions in Thiol Protection and Redox Regulation of the Glyceraldehyde-3-Phosphate Dehydrogenase Gap in Staphylococcus aureus Under Hypochlorite Stress. *Antioxid. Redox Signal.* **2018**, *28*, 410–430. [CrossRef] [PubMed]
24. Tsuji, K.; Yoon, K.S.; Ogo, S. Glyceraldehyde-3-phosphate dehydrogenase from Citrobacter sp. S-77 is post-translationally modified by CoA (protein CoAlation) under oxidative stress. *FEBS Open Bio* **2019**, *9*, 53–73. [CrossRef]
25. Nakajima, H.; Amano, W.; Fujita, A.; Fukuhara, A.; Azuma, Y.T.; Hata, F.; Inui, T.; Takeuchi, T. The active site cysteine of the proapoptotic protein glyceraldehyde-3-phosphate dehydrogenase is essential in oxidative stress-induced aggregation and cell death. *J. Biol. Chem.* **2007**, *282*. [CrossRef] [PubMed]
26. Minor, W.; Cymborowski, M.; Otwinowski, Z.; Chruszcz, M. HKL-3000: The integration of data reduction and structure solution-from diffraction images to an initial model in minutes. *Acta Crystallogr. D* **2006**, *62*, 859–866. [CrossRef] [PubMed]

27. Evans, P. Scaling and assessment of data quality. *Acta Crystallogr. Sect. D Struct. Biol.* **2006**, *62*, 72–82. [CrossRef] [PubMed]
28. Terwilliger, T.C.; Adams, P.D.; Read, R.J.; Mccoy, A.J.; Moriarty, N.W.; Grosse-Kunstleve, R.W.; Afonine, P.V.; Zwart, P.H.; Hung, L.W. Decision-making in structure solution using Bayesian estimates of map quality: The PHENIX AutoSol wizard. *Acta Crystallogr. D* **2009**, *65*, 582–601. [CrossRef]
29. Emsley, P.; Cowtan, K. Coot: Model-building tools for molecular graphics. *Acta Crystallogr. D* **2004**, *60*, 2126–2132. [CrossRef]
30. Bunkoczi, G.; Echols, N.; McCoy, A.J.; Oeffner, R.D.; Adams, P.D.; Read, R.J. Phaser.MRage: Automated molecular replacement. *Acta Crystallogr. Sect. D Struct. Biol.* **2013**, *69*, 2276–2286. [CrossRef]
31. Afonine, P.V.; Grosse-Kunstleve, R.W.; Echols, N.; Headd, J.J.; Moriarty, N.W.; Mustyakimov, M.; Terwilliger, T.C.; Urzhumtsev, A.; Zwart, P.H.; Adams, P.D. Towards automated crystallographic structure refinement with phenix.refine. *Acta Crystallogr. Sect. D Struct. Biol.* **2012**, *68*, 352–367. [CrossRef]
32. Sierra-Gomez, Y.; Rodriguez-Hernandez, A.; Cano-Sanchez, P.; Gomez-Velasco, H.; Hernandez-Santoyo, A.; Siliqi, D.; Rodriguez-Romero, A. A biophysical and structural study of two chitinases from Agave tequilana and their potential role as defense proteins. *FEBS J.* **2019**. [CrossRef] [PubMed]
33. Kim, Y.J. A cryoprotectant induces conformational change in glyceraldehyde-3-phosphate dehydrogenase. *Acta Crystallogr. Sect. F Struct. Biol. Commun.* **2018**, *74*, 277–282. [CrossRef] [PubMed]
34. Sirover, M.A. Structural analysis of glyceraldehyde-3-phosphate dehydrogenase functional diversity. *Int. J. Biochem. Cell B* **2014**, *57*, 20–26. [CrossRef] [PubMed]
35. Bedhomme, M.; Adamo, M.; Marchand, C.H.; Couturier, J.; Rouhier, N.; Lemaire, S.D.; Zaffagnini, M.; Trost, P. Glutathionylation of cytosolic glyceraldehyde-3-phosphate dehydrogenase from the model plant Arabidopsis thaliana is reversed by both glutaredoxins and thioredoxins in vitro. *Biochem. J.* **2012**, *445*, 337–347. [CrossRef] [PubMed]
36. Muronetz, V.I.; Melnikova, A.K.; Saso, L.; Schmalhausen, E.V. Influence of Oxidative Stress on Catalytic and Non-glycolytic Functions of Glyceraldehyde-3-phosphate dehydrogenase. *Curr. Med. Chem.* **2018**. [CrossRef]
37. Hoffmann, F.; Rinas, U. Stress induced by recombinant protein production in Escherichia coli. *Adv. Biochem. Eng. Biotechnol.* **2004**, *89*, 73–92.
38. Duee, E.; OlivierDeyris, L.; Fanchon, E.; Corbier, C.; Branlant, G.; Dideberg, O. Comparison of the structures of wild-type and a N313T mutant of Escherichia coli glyceraldehyde 3-phosphate dehydrogenases: Implication for NAD binding and cooperativity. *J. Mol. Biol.* **1996**, *257*, 814–838. [CrossRef]
39. Wang, H.B.; Wang, M.J.; Yang, X.M.; Xu, X.H.; Hao, Q.; Yan, A.X.; Hu, M.L.; Lobinski, R.; Li, H.Y.; Sun, H.Z. Antimicrobial silver targets glyceraldehyde-3-phosphate dehydrogenase in glycolysis of E. coli. *Chem. Sci.* **2019**, *10*, 7193–7199. [CrossRef]
40. Patel, D.K.; Shah, K.R.; Pappachan, A.; Gupta, S.; Singh, D.D. Cloning, expression and characterization of a mucin-binding GAPDH from Lactobacillus acidophilus. *Int. J. Biol. Macromol.* **2016**, *91*, 338–346. [CrossRef]
41. Terrasse, R.; Amoroso, A.; Vernet, T.; Di Guilmi, A.M. Streptococcus pneumoniae GAPDH Is Released by Cell Lysis and Interacts with Peptidoglycan. *PLoS ONE* **2015**, *10*, e0125377. [CrossRef]
42. Perez-Casal, J.; Potter, A.A. Glyceradehyde-3-phosphate dehydrogenase as a suitable vaccine candidate for protection against bacterial and parasitic diseases. *Vaccine* **2016**, *34*, 1012–1017. [CrossRef] [PubMed]
43. Gerszon, J.; Rodacka, A. Oxidatively modified glyceraldehyde-3-phosphate dehydrogenase in neurodegenerative processes and the role of low molecular weight compounds in counteracting its aggregation and nuclear translocation. *Ageing Res. Rev.* **2018**, *48*, 21–31. [CrossRef] [PubMed]
44. Muronetz, V.I.; Barinova, K.V.; Stroylova, Y.Y.; Semenyuk, P.I.; Schmalhausen, E.V. Glyceraldehyde-3-phosphate dehydrogenase: Aggregation mechanisms and impact on amyloid neurodegenerative diseases. *Int. J. Biol. Macromol.* **2017**, *100*, 55–66. [CrossRef] [PubMed]
45. Eby, D.; Kirtley, M.E. Role of Lysine Residues in the Binding of Glyceraldehyde-3-Phosphate Dehydrogenase to Human-Erythrocyte Membranes. *Biochem. Biophys. Res. Commun.* **1983**, *116*, 423–427. [CrossRef]
46. Hara, M.R.; Agrawal, N.; Kim, S.F.; Cascio, M.B.; Fujimuro, M.; Ozeki, Y.; Takahashi, M.; Cheah, J.H.; Tankou, S.K.; Hester, L.D.; et al. S-nitrosylated GAPDH initiates apoptotic cell death by nuclear translocation following Siah1 binding. *Nat. Cell Biol.* **2005**, *7*, 665–674. [CrossRef]

47. Hillion, M.; Imber, M.; Pedre, B.; Bernhardt, J.; Saleh, M.; Van Loi, V.; Maass, S.; Becher, D.; Rosado, L.A.; Adrian, L.; et al. The glyceraldehyde-3-phosphate dehydrogenase GapDH of Corynebacterium diphtheriae is redox-controlled by protein S-mycothiolation under oxidative stress. *Sci. Rep. UK* **2017**, *7*. [CrossRef]
48. Arutyunova, E.I.; Danshina, P.V.; Domnina, L.V.; Pleten, A.P.; Muronetz, V.I. Oxidation of glyceraidehyde-3-phosphate dehydrogenase enhances its binding to nucleic acids. *Biochem. Biophys. Res. Commun.* **2003**, *307*, 547–552. [CrossRef]
49. Frayne, J.; Taylor, A.; Cameron, G.; Hadfield, A.T. Structure of Insoluble Rat Sperm Glyceraldehyde-3-phosphate Dehydrogenase (GAPDH) via Heterotetramer Formation with Escherichia coli GAPDH Reveals Target for Contraceptive Design. *J. Biol. Chem.* **2009**, *284*, 22703–22712. [CrossRef]